A&A 668, A152 (2022)
https://doi.org/10.1051/0004-6361/202244648

Astronomy & Astrophysics

Detection of minute-timescale γ-ray variability in BL Lacertae by *Fermi*-LAT

A. Pandey and C. S. Stalin

Indian Institute of Astrophysics, Block II, 100 Feet Rd, Koramangala, Bangalore, Karnataka 560034, India
e-mail: ashwanitapan@gmail.com

Received 1 August 2022 / Accepted 29 September 2022

ABSTRACT

BL Lacertae, the prototype of the BL Lacertae (BL Lac) category of blazars, underwent a giant γ-ray flare in April 2021. The Large Area Telescope (LAT) on board the *Fermi* Gamma-ray Space Telescope (hereafter *Fermi*-LAT) observed a peak γ-ray (0.1−500 GeV) flux of $\sim 2 \times 10^{-5}$ ph cm^{-2} s^{-1} within a single orbit on 2021 April 27, which is historically the brightest γ-ray flux ever detected from the source. Here, we report, for the first time, the detection of significant minute-timescale GeV γ-ray flux variability in the BL Lac subclass of blazars by the *Fermi*-LAT. We resolved the source variability down to two-minute binned timescales with a flux halving time of ∼1 min, which is the shortest GeV variability timescale ever observed from blazars. The detected variability timescale is much shorter than the light-crossing time (∼14 min) across the central black hole of BL Lac, indicating a very compact γ-ray emission site within the outflowing jet. Such a compact emitting region requires the bulk Lorentz factor of the jet to be larger than 16 so that the jet power is not super Eddington. We found a minimum Doppler factor $\delta_{\rm min}$ of 15 using the δ function approximation for the $\gamma\gamma$ opacity constraint. For a conical jet geometry, considering $\Gamma = \delta_{\rm min}$, the observed short variability timescale for BL Lac suggests that the very compact emission region lies at a distance of about 8.62×10^{14} cm from its central engine.

Key words. galaxies: active – BL Lacertae objects: individual: BL Lacertae – BL Lacertae objects: general

1. Introduction

The extragalactic γ-ray sky is dominated by the blazar category of active galactic nuclei (AGN; Abdollahi et al. 2020). Blazars, comprising flat-spectrum radio quasars (FSRQs) and BL Lac objects (BL Lacs), are radio-loud AGN that have their relativistic jets aligned close to the line of sight to the observer (Blandford 1978; Urry & Padovani 1995). They emit most of their energy in high-energy γ-rays with the most powerful sources, during strong flares, reaching γ-ray luminosities (in the isotropic emission scenario) as high as $L_\gamma \sim 10^{49-50}$ erg s^{-1} (Aharonian et al. 2017b). The broadband spectral energy distributions (SEDs) of blazars have double-hump structures (Fossati et al. 1998). The low-energy component of the SED is well explained by synchrotron emission from the relativistic electrons within the jet, while the origin of the high-energy component is still unclear (e.g. Böttcher 2007). One of the mechanisms responsible for the high-energy γ-ray radiation is the synchrotron self-Compton (SSC) process by which the synchrotron photons emitted by the relativistic electrons in the jet are Compton up-scattered by the same population of electrons in the jet (Maraschi et al. 1992). An alternative model posits the production of γ-rays by inverse Compton scattering of seed photons external to the jet, by electrons in the emitting jet. The seed photons could be the ultraviolet photons from the accretion disk (Dermer & Schlickeiser 1993), the photons from emission lines from the broad-line region (Sikora et al. 1994), and/or the infrared emission from the dusty torus (Błażejowski et al. 2000). Alternatively, hadronic processes could also produce γ-rays (Böttcher et al. 2013). Based on the synchrotron peak frequency ($\nu_{\rm peak}$) of their SEDs, BL Lacs are further divided into low-frequency peaked BL Lacs (LBLs; $\nu_{\rm peak} \leq 10^{14}$ Hz), intermediate-frequency peaked BL Lacs (IBLs; 10^{14} Hz $< \nu_{\rm peak} < 10^{15}$ Hz), and high-frequency peaked BL Lacs (HBLs; $\nu_{\rm peak} \geq 10^{15}$ Hz; Padovani & Giommi 1995; Abdo et al. 2010a).

The γ-rays from blazars are known to be highly variable (Abdo et al. 2010b; Rajput et al. 2020), which indicates the emission region is highly compact (Fichtel et al. 1994) and the γ-ray radiation is highly beamed (Dondi & Ghisellini 1995). However, the exact physical processes that are responsible for the generation of the observed γ-ray emission, as well as their production site, are uncertain and highly debated. Using powerful observational facilities in the γ-ray domain, rapid γ-ray variations have been detected in seven AGN so far, including three BL Lacs (PKS 2155−304 Aharonian et al. 2007a, Mrk 501 Albert et al. 2007, BL Lac Arlen et al. 2013; MAGIC Collaboration 2019), three FSRQs (PKS 1222+21 Aleksić et al. 2011, 3C 279 Ackermann et al. 2016, CTA 102 Ackermann et al. 2016), and one radio galaxy (IC 310 Aleksić et al. 2014). However, the minute-timescale γ-ray variations were also detected multiple times in the same source. For example, Arlen et al. (2013) observed a rapid TeV γ-ray flare from BL Lac with an exponential decay time of 13 ± 4 min, and recently MAGIC Collaboration (2019) also reported the detection of a very high energy (VHE) γ-ray flare with a halving time of 26 ± 8 min from the same source. Moreover, the majority of the findings of rapid γ-ray variations come from VHE observations by the ground-based Cerenkov telescopes, except for two sources, namely 3C 279 (Ackermann et al. 2016) and CTA 102 (Shukla et al. 2018), where the short-timescale variations are from the GeV observations by the *Fermi*-LAT. Both of these sources belong to the FSRQ subclass of blazars. To date, no rapid GeV γ-ray variability has been detected in any of the BL Lacs by the *Fermi*-LAT.

The abundant data from *Fermi*-LAT (Atwood et al. 2009) observations provide ample opportunity to find evidence of short-timescale variations in more blazars. Our motivation here is to find rapid γ-ray variations in the BL Lac subclass of blazars using the *Fermi*-LAT observations. BL Lac, at a redshift of $z = 0.069$ (Miller et al. 1978), is an eponym of the BL Lac category of blazars. It is usually categorised as an LBL (Nilsson et al. 2018), but sometimes it is also classified as an IBL (Ackermann et al. 2011). During April 2021, the *Fermi*-LAT observed the largest γ-ray flare from BL Lac seen to date, which allowed us to search for the rapid γ-ray variations in the source. In this work, we report the first-ever detection of minute-timescale γ-ray variability in any BL Lac object by *Fermi*-LAT.

This paper is organised as follows. In Sect. 2 we give an overview of observations and the data analysis of *Fermi*-LAT. Results of our rapid γ-ray variability study are given in Sect. 3, we provide a discussion in Sect. 4, and present a summary of our findings in this study in Sect. 5.

2. Observations and data analysis

2.1. Gamma-ray observations

We used the Pass 8 (P8R3) *Fermi*-LAT γ-ray (0.1−500 GeV) data of BL Lac from MJD 59305 (2021 April 1) to MJD 59340 (2021 May 6). We analysed the data following the standard LAT data-analysis procedures[1] and using the `FermiTool` software package version 2.0.8 with the `P8R3_SOURCE_V3` instrument response functions. For our analysis, we chose all the SOURCE class events (evclass = 128 and evtype = 3) within a circular region of 10° (region of interest; ROI) around the blazar BL Lac. To select the good time intervals, we used a filter "(DATA_QUAL>0)&&(LAT_CONFIG==1)" and applied a maximum zenith-angle cut of 90° to avoid the background γ-rays from the Earth's limb. We employed the unbinned maximum likelihood optimisation technique for flux determination and spectral modelling (Abdo et al. 2009). Our model file includes all the sources from the *Fermi*-LAT Fourth Source catalogue (4FGL; Abdollahi et al. 2020) within 20° of the source as well as the Galactic and extragalactic isotropic diffuse emission components[2]. During the initial likelihood fit, all the parameters of the sources lying outside the ROI were kept fixed to their values in 4FGL, while the normalisation and the spectral parameters of the sources within the ROI were left to vary freely. The normalisations of the diffuse emission components were also left free.

2.2. X-ray observations

We generated the X-ray spectrum of BL Lac using the online *Swift*-XRT data products generator tool[3] (for details, see Evans et al. 2009). This tool produces the pile-up corrected source spectrum, the background spectrum, and the response files using the HEASOFT version 6.29. The X-ray spectrum of BL Lac was fitted with an absorbed power-law (PL) model in the XSPEC version 12.12.0 to obtain the 0.3−10 keV X-ray flux and the photon index. For the fitting, we assumed a fixed Galactic hydrogen column density of $n_{\rm H} = 3.03 \times 10^{21}$ cm^{-2} (Willingale et al. 2013).

[1] https://fermi.gsfc.nasa.gov/ssc/data/analysis/
[2] `gll_iem_v07` and `iso_P8R3_SOURCE_V3_v1`, respectively.
[3] https://www.swift.ac.uk/user_objects/

3. Results

3.1. γ-ray light curve

Figure 1 presents the γ-ray light curves of BL Lac for a period of about one month, which includes the brightest outburst observed on 2021 April 27. Although the spectral shape of BL Lac is defined as log-parabola (LP) in the 4FGL catalogue (Abdollahi et al. 2020), we generated the light curves by modelling the spectra in each time bin as a simple PL, because the PL indices have smaller statistical uncertainties than those obtained from the complex LP model (e.g. Abdo et al. 2011). Also, choosing a simple PL model is more appropriate for this work as we are probing the shortest timescale γ-ray variations, and are therefore dealing with smaller photon statistics. The arrival time and the energy of the highest energy photon (bottom panel) coming from the source were derived using the tool `gtsrcprob` on ULTRACLEAN event class (evclass = 512).

The maximum one-day averaged flux (above 100 MeV) was observed on MJD 59331 (2021 April 27) reaching $(6.8 \pm 0.3) \times 10^{-6}$ ph cm^{-2} s^{-1}, which is the highest daily binned flux ever observed from this source. The photon index corresponding to this highest flux is 1.90 ± 0.03, which is slightly harder than the value (2.2025) mentioned in the 4FGL catalogue. The three-hour binned γ-ray light curve of BL Lac shown in panel c of Fig. 1 indicates two sharp γ-ray flares.

To investigate any instrumental uncertainties in the analysis, we also generated the daily binned light curves of BL Lac in 0.1−1 GeV, 1−50 GeV, and 50−500 GeV energy bands for the period considered. As seen in Fig. 2, the light curves in those three energy bands follow a pattern similar to the total 0.1−500 GeV energy band light curve. There are only six data points in the 50−500 GeV light curve as the source was not significantly (TS > 9) detected in this energy range in the other time bins.

The highest-energy photon, 128 GeV, was recorded with >99.99% probability on MJD 59333 (2021 April 29), which is in the declining phase of the main flare. A similar trend was also seen in 3C 279 where the highest energy photon was observed at the end of the outburst phase (Ackermann et al. 2016).

3.2. Suborbital timescale variability

As shown in panel c of Fig. 1, the source flux exceeded the value of 10^{-5} ph cm^{-2} s^{-1} on two days, namely 2021 April 23 (MJD 59327) and 2021 April 27 (MJD 59331) on three occasions with high photon statistics; MJD 59327.18756 (TS = 798.985), MJD 59331.18756 (TS = 1968.951), and MJD 59331.31256 (TS = 776.058). This allowed us to further resolve the light curve with shorter timescales on these two days. We first generated the light curves with bin size equal to the orbital period (∼95.4 min) of the *Fermi*-LAT. The orbit-binned light curves of BL Lac on 2021 April 23 (left) and April 27 (right) are shown in the top panels of Fig. 3. We estimated the shortest flux doubling/halving timescales on these two epochs, as follows:

$$F(t_2) = F(t_1) \times 2^{\Delta t/\tau}. \quad (1)$$

Here, $F(t_1)$ and $F(t_2)$ are the flux values at times t_1 and t_2, respectively, $\Delta t = t_2 - t_1$, and τ denotes the flux doubling/halving timescale. We observed a flux halving timescale of $\sim(0.68 \pm 0.22)$ h with a significance of $\sim 4\sigma$ during the decay of the flare on MJD 59327. We also detected a flux doubling timescale of $\sim(1.14 \pm 0.21)$ h with $\sim 6\sigma$ significance during the rise of the flare on MJD 59331.

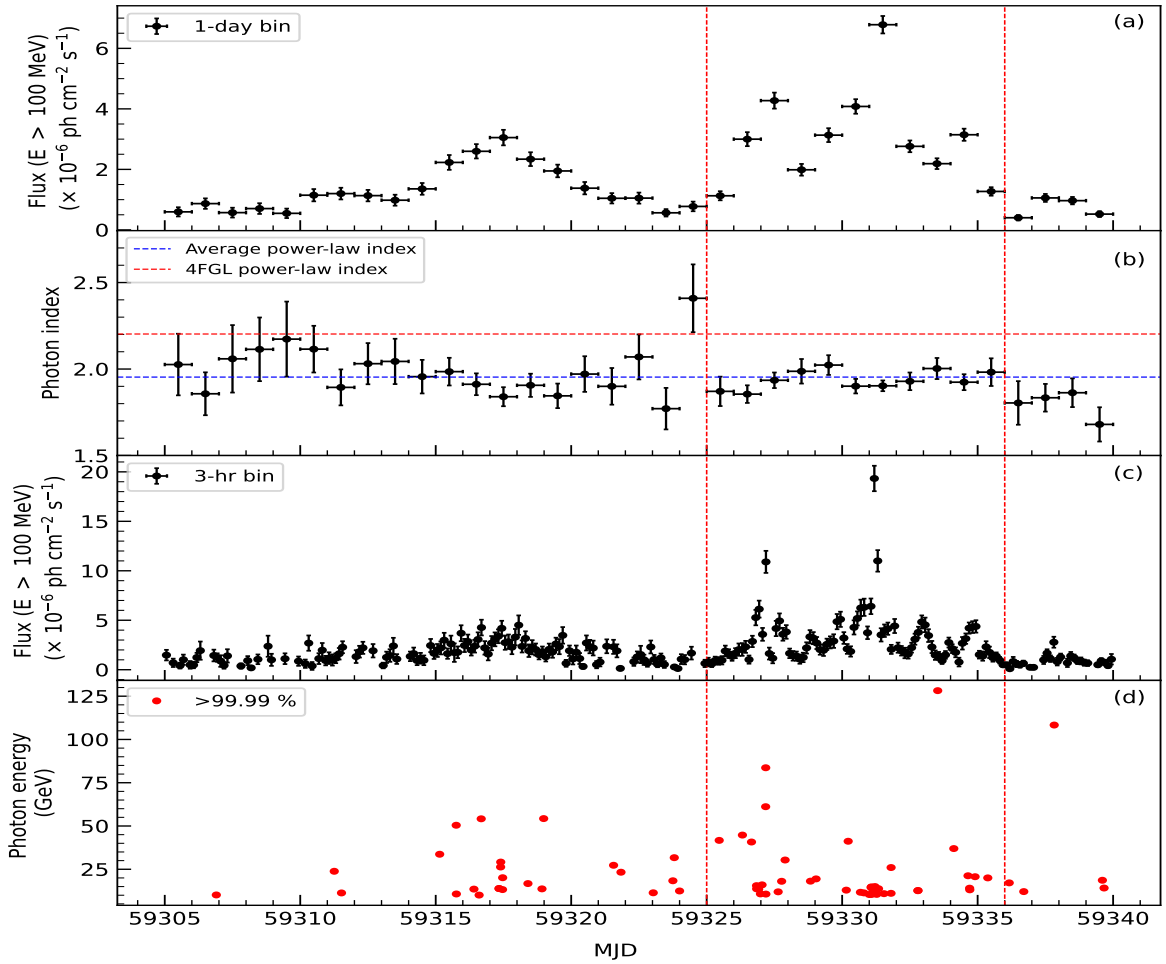

Fig. 1. *Fermi*-LAT light curves of BL Lac covering a period of ∼35 days. *Panel a*: one-day binned γ-ray (0.1−500 GeV) light curve. *Panel b*: variation of γ-ray photon index with time; the blue and red horizontal lines indicate the average PL index during the period considered and the PL index mentioned in the 4FGL catalogue, respectively. *Panel c*: three-hour binned γ-ray light curve of BL Lac. *Panel d*: arrival time distribution of photons with energies greater than 10 GeV. The vertical red lines indicate the period of the major γ-ray flare.

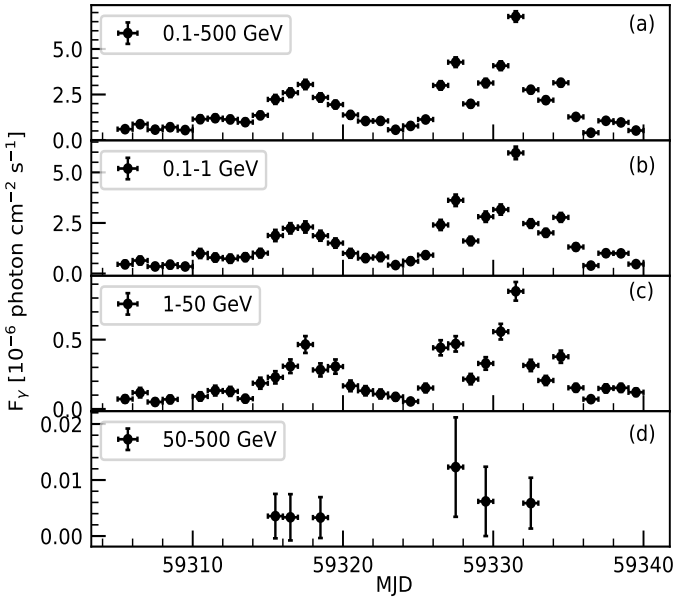

Fig. 2. Daily-averaged γ-ray light curves of BL Lac in different energy bands. The energy range used to generate the light curve is mentioned in each panel.

To understand the temporal evolution of the flux, we fitted the peaks of orbit-binned light curves by a function of the sum of the exponential defined as (Abdo et al. 2010b)

$$F(t) = 2F_0 \left(e^{\frac{t_0 - t}{T_r}} + e^{\frac{t - t_0}{T_d}} \right)^{-1} . \quad (2)$$

Here, F_0 is the flux value at time t_0 denoting the flare amplitude, T_r is the rise time, and T_d is the decay time of the flare. The results of the fit are given in Table 1. We also estimated a parameter $\xi = (T_d - T_r)/(T_d + T_r)$, which describes the symmetry of the flares (Abdo et al. 2010b). For both the flares, we found $-0.3 < \xi < 0.3$, implying that these flares are symmetric.

Rapid flux variations with high photon statistics observed on MJD 59327 and MJD 59331 provide us with an opportunity to examine ultra-fast flux variations on the timescale of a few minutes. To detect such rapid flux variations, we generated two-minute, three-minute, and five-minute binned light curves for each orbit on these two days. Similar to Ackermann et al. (2016) and Shukla et al. (2018), we searched for minute-scale variability on these two days by fitting a constant flux to each orbit for all three time bins and subsequently computing the probability (p-value) of finding a constant flux. As detections of minute-timescale γ-ray variations are very rare, we

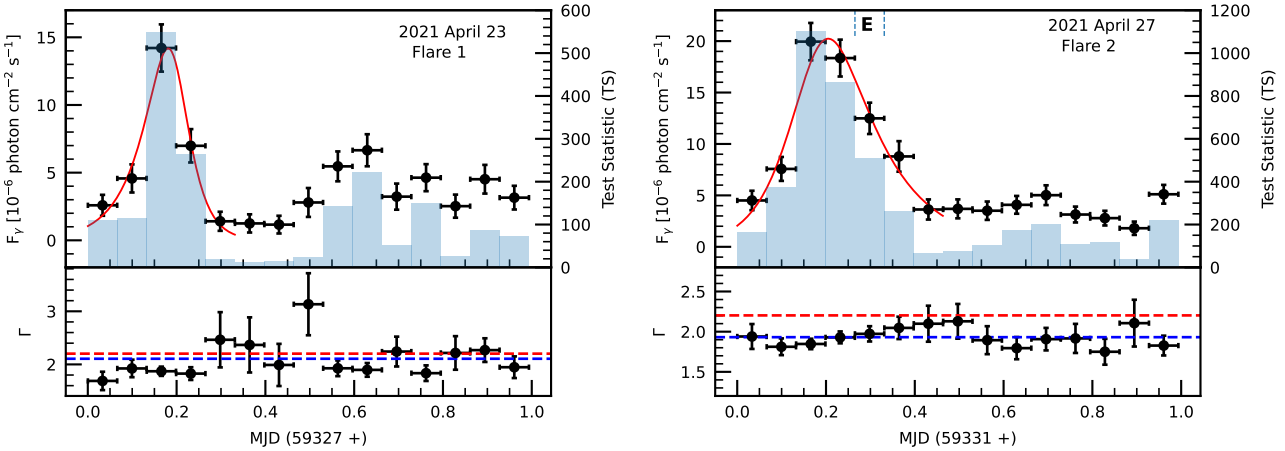

Fig. 3. Orbit-binned γ-ray light curves of BL Lac for 2021 April 23 (*left*) and 2021 April 27 (*right*). The TS values for each time bin in both the light curves are shown as blue bars. The PL index for each bin is plotted in the *bottom panels*. The red and blue horizontal lines in the *bottom panels* represent the 4FGL PL index (2.2025) and the average photon index on that day, respectively.

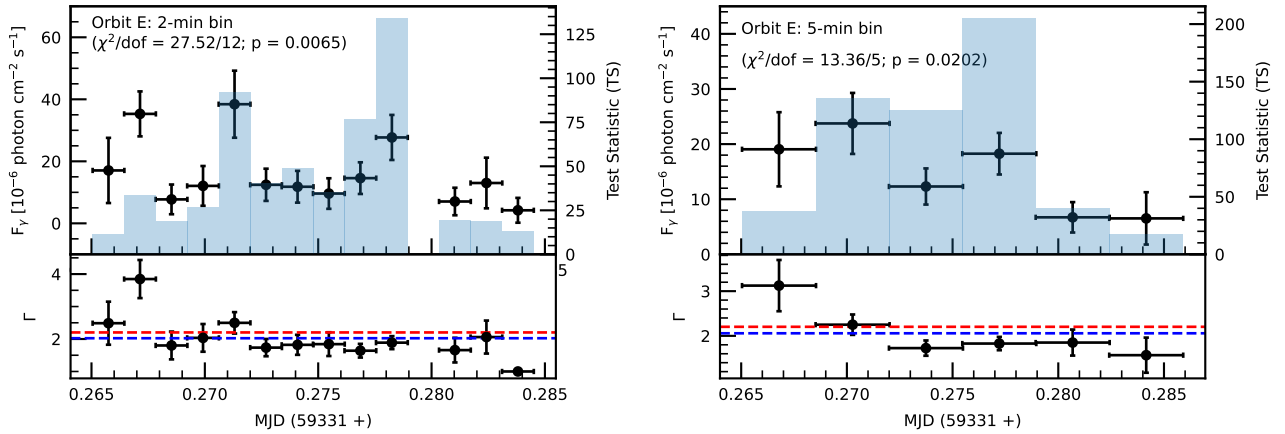

Fig. 4. Sub-orbital light curves of BL Lac. *Top panels*: are the two-minute (*left*) and five-minute (*right*) binned light curves for the orbit E. The TS values for each time bin in both the light curves are shown as blue bars. The PL index for each bin is plotted in the *bottom panels*. The red and blue horizontal lines in the *bottom panels* represent the 4FGL PL index (2.2025) and the average photon index on that day, respectively.

Table 1. Results of the sum of the exponential fit to the orbit-binned light curves.

Flare	Peak time (MJD)	Peak flux ($\times 10^{-6}$ ph cm^{-2} s^{-1})	Rise time (T_r)	Decay time (T_d)	ξ
Flare 1	59327.19 ± 0.02	13.61 ± 1.84	1.42 ± 0.32 h	0.79 ± 0.27 h	−0.28
Flare 2	59331.18 ± 0.02	19.47 ± 1.67	1.49 ± 0.29 h	2.63 ± 0.47 h	0.28

conservatively chose a 95% confidence level (p-value smaller than 0.05) as the detection limit for suborbital variability. On MJD 59327, the p-values for all the orbits and for all the time bins are found to be consistent with constant flux. Similarly, on MJD 59331, for all the orbits, except orbit E, we obtained p-values denoting no flux variations for all the time bins. For orbit E, we detected minute-scale variability in the two-minute binned ($p = 0.0065$, χ^2/d.o.f. = 27.52/12) and five-minute binned ($p = 0.0202$, χ^2/d.o.f. = 13.36/5) light curves. However, in the three-min binned light curve of orbit E, the variations were not significant ($p = 0.6339$, χ^2/d.o.f. = 6.12/8). Our p-values are comparable to those found by Ackermann et al. (2016) in a single orbit during a giant flare of blazar 3C 279. The two-minute binned and five-minute binned light curves for orbit E are shown in the top panels of Fig. 4. We also searched for the flux doubling/halving timescales in these light curves using Eq. (1). We found a halving timescale of $\sim(1 \pm 0.3)$ min with $\sim 3.2\sigma$ in the two-minute binned light curve of orbit E.

3.3. Gamma-ray spectral variability

We investigated the γ-ray spectral variability of BL Lac on different time bins, namely daily, orbital, and shortest time bins. For all the time bins, the average PL photon indices are somewhat harder than its value (2.2025) in the 4FGL catalogue. The average PL photon indices for these time bins are given in Table 2. We also searched for any correlation between the observed γ-ray flux and the PL index in these time bins using the Pearson correlation. The results of the correlation study are given in Table 2. As seen from Table 2, no significant correlation

Table 2. Results of spectral variability of BL Lac in different time bins.

Bin size	Average PL index	Flux vs. PL index	
		r	p
1-day	1.95 ± 0.02	−0.16	0.349
1-orbit (flare 1)	2.11 ± 0.08	−0.38	0.161
1-orbit (flare 2)	1.93 ± 0.04	−0.14	0.622
2-min (orbit E)	2.02 ± 0.11	0.76	0.003
5-min (orbit E)	2.06 ± 0.14	0.59	0.209

Notes. Here, r and p represent the Pearson correlation coefficient and the null-hypothesis probability, respectively.

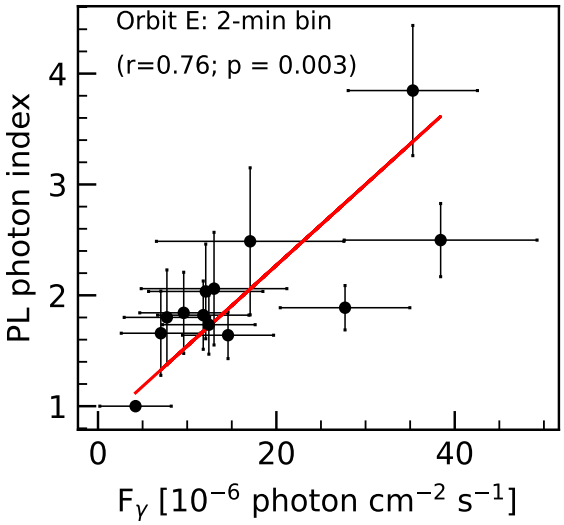

Fig. 5. Variation of PL photon index with γ-ray flux for the two-minute binned light curve of orbit E. A softer-when-brighter trend is clearly visible.

was found between the γ-ray flux and PL index in any of the time bins except in the two-minute time bin. We found a significant ($p < 0.01$) positive correlation between γ-ray flux and PL index in the two-minute binned light curve indicating a softer-when-brighter trend. The variation of PL photon index with γ-ray flux for the two-minute binned light curve of orbit E is shown in Fig. 5.

4. Discussion

This is the first time that rapid (minute-timescale) γ-ray variability has been detected in any BL Lac category of blazars by *Fermi*-LAT. We observed significant variations in the minute-scale binned γ-ray light curves with a halving timescale of ∼1 min during the historically bright γ-ray flare from BL Lac on MJD 59331. The detection of such a rapid variability timescale challenges the existing γ-ray emission models.

The black hole mass for BL Lacertae is $1.7 \times 10^8\,M_\odot$ (Zamaninasab et al. 2014) and the corresponding event horizon light-crossing time is ∼14 min. The detected variability timescale (∼1 min) is much shorter than the event horizon light-crossing time, indicating that the enhanced γ-ray emission is coming from a very compact region within the jet. Such rapid variations could be triggered either by dissipation in a small fraction of the black hole magnetosphere at the base of the jet or by small-scale instabilities within the jet (Begelman et al. 2008). Alternatively, the jet could be much more extended and the emission may be coming come from a localised region in the jet that is much smaller than the width of the jet itself. In this scenario, the innermost region of the jet at the subparsec level is also responsible for the observed GeV emission.

The total jet power that is required to produce the observed γ-ray luminosity $L_\gamma \sim 5 \times 10^{47}$ erg s^{-1} is $L_j \simeq L_\gamma/(\eta_j \Gamma^2)$, where $\eta_j \sim 0.1$ is the radiative jet efficiency (Ackermann et al. 2016). The jet power should be less than the Eddington luminosity $L_{Edd} \sim 2 \times 10^{46}$ erg s^{-1} which implies that $\Gamma > 16$.

The minimum Doppler factor, δ_{min}, of the γ-ray emission region can also be estimated numerically using a δ-function approximation for the $\gamma\gamma$ opacity constraint and the detected high-energy γ-ray photons (Dondi & Ghisellini 1995; Ackermann et al. 2010). Assuming that the γ-rays are produced via the SSC scattering process and the target photons for SSC are X-ray photons, a lower limit of the Doppler factor can be calculated as

$$\delta_{min} = \left[\frac{\sigma_T d_L^2 (1+z)^2 f_\epsilon E_1}{4\tau m_e c^4}\right]^{1/6}, \quad (3)$$

where σ_T is the Thomson scattering cross section, $d_L = 307$ Mpc is the luminosity distance[4] for BL Lac, $f_\epsilon = 7 \times 10^{-11}$ erg cm^{-2} s^{-1} is the X-ray flux obtained from the *Swift*-XRT observation (obsid 00034748061; X-ray photon index $= 2.28 \pm 0.08$), and $E_1 = 26\,\mathrm{GeV}/m_e c^2$ is the highest energy photon. We estimated δ_{min} to be ∼15, which is consistent with the $\delta_{min} = 13$–17 obtained by Arlen et al. (2013).

Taking $\delta = 16$, the detected size of the γ-ray-emitting region $R \leq c\tau(\delta/(1+z)) \leq 2.69 \times 10^{13}$ cm. For a conical geometry of the jet, the distance of the γ-ray emission region from the central super-massive black hole is $D \leq (2c\Gamma^2\tau)/(1+z) \approx 8.62 \times 10^{14}$ cm, assuming $\Gamma = \delta_{min}$ (Abdo et al. 2011). Flares seen on the orbit-binned light curves have a symmetric profile and can therefore be associated with the crossing time of radiation through the emitting region or can be explained by the superposition of several short-duration flares (Abdo et al. 2010b).

5. Summary

In this work, we report the first detection of minute-timescale GeV γ-ray variability in the BL Lac category of blazars by *Fermi*-LAT. We detected a flux halving timescale of ∼1 min from BL Lacertae on 2021 April 27. This observed short timescale of variability requires a minimum bulk Lorentz factor of 16 for the jet power to be less than the Eddington value. Also, the $\gamma\gamma$ transparency argument for that epoch of short-timescale variability detection requires a minimum Doppler factor of ∼15. We find a softer-when-brighter trend in the two-minute binned light curve of orbit E.

Acknowledgements. We thank the referee for his/her critical comments that helped in the improvement of the manuscript. We thank Dr. Vaidehi S. Paliya for a fruitful scientific discussion. This work has made use of *Fermi* data collected from the *Fermi* Science Support Center (FSSC) supported by the NASA Goddard Space Flight Center. This research has made use of the High-Performance Computing (HPC) resources (https://www.iiap.res.in/?q=facilities/computing/nova) made available by the Computer Center of the Indian Institute of Astrophysics, Bangalore. This work made use of data supplied by the UK Swift Science Data Centre at the University of Leicester.

[4] Assuming $H_0 = 71$ km s^{-1} Mpc, $\Omega_M = 0.27$, $\Omega_\Lambda = 0.73$ (Larson et al. 2011).

References

Abdo, A. A., Ackermann, M., Ajello, M., et al. 2009, ApJS, 183, 46
Abdo, A. A., Ackermann, M., Agudo, I., et al. 2010a, ApJ, 716, 30
Abdo, A. A., Ackermann, M., Ajello, M., et al. 2010b, ApJ, 732, 520
Abdo, A. A., Ackermann, M., Ajello, M., et al. 2011, ApJ, 733, L26
Abdollahi, S., Acero, F., Ackermann, M., et al. 2020, ApJS, 247, 33
Ackermann, M., Asano, K., Atwood, W. B., et al. 2010, ApJ, 716, 1178
Ackermann, M., Ajello, M., Allafort, A., et al. 2011, ApJ, 743, 171
Ackermann, M., Anantua, R., Asano, K., et al. 2016, ApJ, 824, L20
Aharonian, F. A., Akhperjanian, A. G., Bazer-Bachi, A. R., et al. 2007a, ApJ, 664, L71
Aharonian, F. A., Barkov, M. V., & Khangulyan, D. 2017b, ApJ, 841, 61
Albert, J., Aliu, E., Anderhub, H., et al. 2007, ApJ, 669, 862
Aleksić, J., Antonelli, L. A., Antoranz, P., et al. 2011, ApJ, 730, L8
Aleksić, J., Ansoldi, S., Antonelli, L. A., et al. 2014, Science, 346, 1080
Arlen, T., Aune, T., Beilicke, M., et al. 2013, ApJ, 762, 92
Atwood, W. B., Abdo, A. A., Ackermann, M., et al. 2009, ApJ, 697, 1071
Begelman, M. C., Fabian, A. C., & Rees, M. J. 2008, MNRAS, 384, L19
Blandford, R. D., & Rees, M. J. 1978, in BL Lac Objects, ed. A. M. Wolfe (Pittsburgh: University of Pittsburgh), 328
Błażejowski, M., Sikora, M., Moderski, R., & Madejski, G. M. 2000, ApJ, 545, 107
Böttcher, M. 2007, Ap&SS, 307, 69
Böttcher, M., Reimer, A., Sweeney, K., & Prakash, A. 2013, ApJ, 768, 54
Dermer, C. D., & Schlickeiser, R. 1993, ApJ, 416, 458
Dondi, L., & Ghisellini, G. 1995, MNRAS, 273, 583
Evans, P. A., Beardmore, A. P., Page, K. L., et al. 2009, MNRAS, 397, 1177
Fichtel, C. E., Bertsch, D. L., Chiang, J., et al. 1994, ApJS, 94, 551
Fossati, G., Maraschi, L., Celotti, A., Comastri, A., & Ghisellini, G. 1998, MNRAS, 299, 433
Larson, D., Dunkley, J., Hinshaw, G., et al. 2011, ApJS, 192, 16
MAGIC Collaboration (Acciari, V. A., et al.) 2019, A&A, 623, A175
Maraschi, L., Ghisellini, G., & Celotti, A. 1992, ApJ, 397, L5
Miller, J. S., French, H. B., & Hawley, S. A. 1978, ApJ, 219, L85
Nilsson, K., Lindfors, E., Takalo, L. O., et al. 2018, A&A, 620, A185
Padovani, P., & Giommi, P. 1995, ApJ, 444, 567
Rajput, B., Stalin, C. S., & Rakshit, S. 2020, A&A, 634, A80
Shukla, A., Mannheim, K., Patel, S. R., et al. 2018, ApJ, 854, L26
Sikora, M., Begelman, M. C., & Rees, M. J. 1994, ApJ, 421, 153
Urry, C. M., & Padovani, P. 1995, PASP, 107, 803
Willingale, R., Starling, R. L. C., Beardmore, A. P., Tanvir, N. R., & O'Brien, P. T. 2013, MNRAS, 431, 394
Zamaninasab, M., Clausen-Brown, E., Savolainen, T., & Tchekhovskoy, A. 2014, Nature, 510, 126